Design of JUNO Calibration System

someone[1]

[1] School of Physics and Astronomy, Shanghai Jiao Tong University, Shanghai Key Laboratory for Particle Physics and Cosmology, Shanghai, 200240, China

Abstract: Jiangmen Underground Neutrino Observatory (JUNO) is a spherical-tank (35.4 m diameter) neutrino detector filled with 20 kton liquid scintillator. It is located 700 m underground in Jiangmen City, Guangdong province, China. The primary purpose of JUNO is to measure the neutrino mass hierarchy (MH). So a high physics requirement is purposed for both energy scale and resolution. The overall energy resolution should be better than 3% and uncertainty of the energy scale should be less than 1%. In order to achieve this physics requirement, a design of calibration system is purposed. The design includes types of source, geometries of source design, simulation and expected results.

Key words: JUNO,Calibration,Simulation,Radioactive source

1   Introduction

1.1   Motivation of calibration

JUNO is a muti-purpose neutrino detector, and the main purpose of JUNO is to determine the neutrino mass hierarchy. As a medium baseline reactor anti-neutrino detector, 53 km from the Yangjiang and Taishan NPP, it can resolve the MH in the neutrino oscillation. But this requires very high precise measurement on both energy resolution and scale. Based on Ref. [1], the energy resolution of JUNO detector should be better than 3% and the uncertainty of energy scale should be better than 1%.

However, due to the LS transmittance and total reflection at CD boundary, connection bar and so on, the response of detector is not uniform, and the non-uniformity effect will worsen the detector energy resolution, so we need to correct the non-uniformity with calibration system to make the energy resolution good enough to meet the physics requirement. Fig. 11 shows the simulation of 1 MeV e+ uniformly in CD without correction, the energy resolution is ~7%, which doesn't meet the physics requirement of JUNO. So A calibration strategy for non-uniformity correction is very necessary.

The other effect is about energy non-linearity of detector response. The quenching of LS is different for different energy, and even with the same energy, e-, e+ and gamma still have different quenching, so the quenching of LS is energy and particle dependent. Reference to Ref. [1], the incorrect energy scale will give wrong MH sensitivity (increase or decrease). So control of energy scale uncertainty is essential.
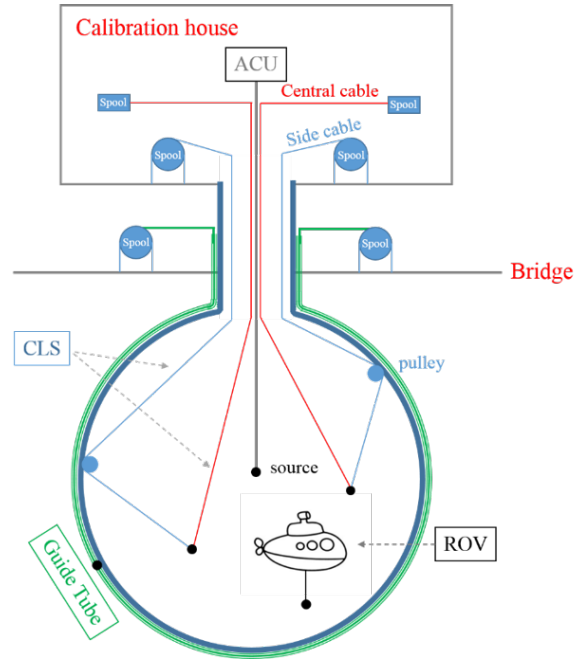
1.2   Calibration system

Fig. 1. The overview of calibration system, including automatic calibration Unit (ACU), cable loop system (CLS), Guide Tube (GT) and Remotely Operated Under-liquid-scintillator Vehicles (ROV)

During the calibration, we need deployment system to move the source to various position. The deployments systems of calibration sources include ACU, CLS, GT, ROV as shown in Fig 1. For ROV and CLS, we will use independent positioning system to determine the position of calibration source.

1) E-mail: someone@sjtu.edu.cn

1.2.1 Automatic Calibration Unit (ACU)

The ACU is developed to do calibration along the central axis of CD, which is very similar to the ACU used in Daya Bay experiment. There are 4 spools installed on the turntable. Three routine sources and one exchangeable source are installed on the ACU. The three routine sources include one gamma source (K40), one neutron source (Am-C) and one laser source. The calibration with ACU can coverage central axis of CD, with high precision of position control. The energy scale of CD can be used with neutron source deployed by ACU to the CD center.

1.2.2 Cable loop system (CLS)

The CLS is necessary since we need to have a better understand of detector non-uniformity. The CLS mainly consist of two cables, side cable and central cable. Controlling the lengths of two cable, we can deploy the sources to scan one vertical plane area. Two sets of CLS with different anchor positions are purposed to increase the scanning area.

1.2.3 Guide Tube (GT)

Since the source cannot reach some boundary area of CD duo to mechanical limit, a Guide Tube calibration system was purposed. The guide tube will be out of CD. With the GT, we can position the calibration source along the surface of CD to obtain a better understand of boundary effect.

1.2.4 Remotely Operated Under-liquid-scintillator Vehicles (ROV)

ROV is 3D scanning system, meaning that we can move the calibration source to nearly everywhere in the CD. ROV is not a routine calibration system, but it still essential as a supplement of ACU, CLS, and GT.

1.2.5 Positioning system

During the non-uniformity correction, we should precisely know the position of calibration points, so it's very important to get the position of calibration source.

However, it's difficult to determine position of source based on length of cable. Due to self-weight, the cable is not straight, we cannot calculate the position of source with naive trigonometric relation. So it's necessary to use independent position system to determine the source position. The requirement of precision of source position is 3 cm compared with that the requirement of vertex reconstruction is 10 cm.

2 Introduce of simulation

2.1 Offline sniper

In this study, we mainly used JUNO official software SNIPER to do simulation. The SNIPER is developed based on Geant4. The framework includes particles generation, detector simulation, calibration and reconstruction, The version of SNIPER used in this study is J17-v1-r1-pre1 released by JUNO software group.

2.2 Introduction of source geometry

The geometries of radioactive source have been written into SNIPER with gdml files. There are three parts for every radioactive source,including source enclosure, weight and quick connector. The total distance from top to bottom is 50 cm, and two cables are used to combine them together. The length of every cable is about 20 cm, which can make sure small shadowing effect from weight and quick connector.

The internal part is stainless steel to seal the source. Both diameter and height of the SS are 6mm, which is very small to decrease the energy loss, with two loops at top and bottom to attach the cable. The outer is the PTFE shell to increase the reflectivity to minimize the photon loss.

The neutron enclosure is different from gamma since smaller neutron source is not safe and necessary. Both diameter and height of neutron source are 8 mm. The source is in a stainless steel (SS) tube. There are two SS pins respectively in top and bottom of the tube. The outer is the PTFE shell just same as gamma source.

2.3 Calibration source

The radioactive sources include routine gamma and neutron sources. The gamma sources have a small size of geometry, with low energy loss and optical shadowing. So we could have a high precise calibration of gamma energy. However, only gamma source is not enough for the high energy calibration. So neutron source is necessary, which can provide 2.22 MeV gamma with neutron captured by hydragen and 4.95 MeV captured by carbon and 6.13 MeV with the second exited stat. The detail of calibration sources and correlated energy is shown in table 1

Table 1. Radioactive sources

Source	Type	Radiation
^{137}Cs	γ	0.662 MeV
^{54}Mn	γ	0.835 MeV
^{60}Co	γ	1.173 + 1.333 MeV
^{40}K	γ	1.461 MeV
^{68}Ge	e^+	annil 0.511 + 0.511 MeV
^{90}Sr	e^-	0~2.28 MeV
^{241}Am-Be	n, γ	neutron + 4.43 MeV
^{241}Am-^{13}C or ^{241}Pu-^{13}C	n, γ	neutron + 6.13 MeV

The Fig. 2 shows the simulation of gamma source Cs-137 with source enclosure. The Compton tail due to energy loss in source geometry will shift the full absorption peak. The fit function will correct the shift.
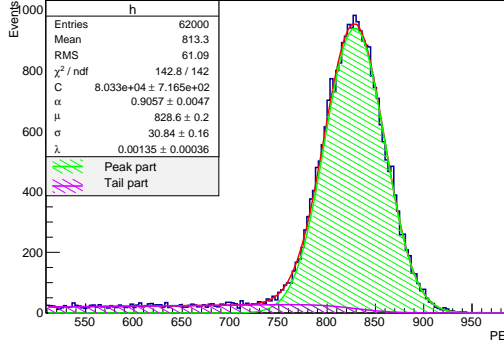
Fig. 2. PE spectrum of Cs137 with source enclosure at CD center.Fit the spectrum with physically-motivated EM calorimeter function in Ref. [4] to obtain full absorption peak. The function can correct the shift of peak by Compton tail.
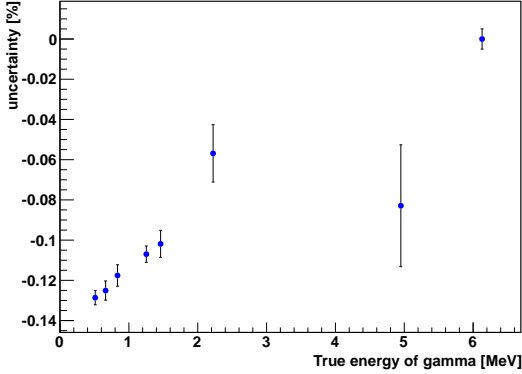

Fig. 3. Optical shadowing effect. The shadowing effect is mainly due to source enclosure and weights. The bias due to shadowing is less than 0.15% for every source. And the shadowing is obvious energy dependent, which makes sense.
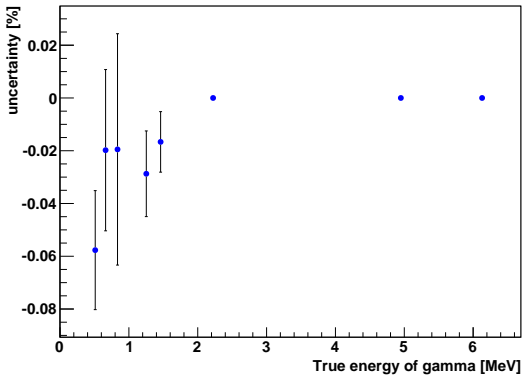

Fig. 4. Compton effect. The Compton effect is also energy dependent even it's not very obvious. Since Co60 has two gammas with average 1.25

MeV energy, it have higher probability of Compton scattring in non-LS compared with single 1.25 MeV gamma.

3 Control energy uncertainty

3.1 Shadowing effect

The material of source container shell is Teflon. Even the reflectivity is very high (assume 90% reflectivity in the simulation), there still must be some optical photon loss. So we need to study the shadowing effect. To decouple the shadowing effect and Compton effect, we can select the events without energy loss during the simulation. With the cut, the PE spectrum follows the Gaussian distribution, so we fit it with Gaussian function to obtain mean value. And then compare it with the ideal case, bare source without enclosure. Fig. 3 shows the uncertainty due to the shadowing effect.

3.2 Compton effect

The Compton effect is due to energy loss in non-LS material, and this will introduce Compton shoulder in PE spectrum. And the Compton shoulder will shift the mean value. Even we use physically-motivated EM calorimeter function in Ref. [4] to correct this effect, there is still some uncertainty we should consider. Fig. 4 the uncertain due to the Compton effect.

3.3 Electronic effect

The non-linearity of electronic can be calibrated with our lased calibration system. The intensity of laser calibration system can be controled to 0.3% uncertainty in Ref. [2], which can give a good calibration for electronic electronic. So in this paper, we roughly assume the uncertainty from electronic non-linearity is 0.3%.

3.4 Statistical effect

Since the requirement of uncertainty is 0.3%, it's better to control the statistical uncertainty less than 0.03%. Based on this, we did the simulation for all the source. We need about 30000 events for every source. For every source calibration, it will take 5 minutes. So the rate of every source should be about 100 Hz.
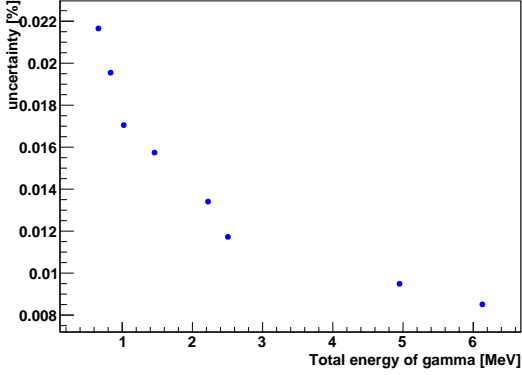
Fig. 5. Statistic uncertainty. The uncertainty is significantly energy dependent, which make sennse.

4 Energy scale

One of main purposes of JUNO calibration is to control uncertainty of the scale less than 1%. In order to reach this physics requirement, we should have a better understanding of the energy non-linearity of detector response. A series of radioactive sources will be used to do the calibration of energy non-linearity, including gamma sources, neutron sources and beta source.

4.1 Energy non-linearity of gamma

Here we will introduce the strategy of JUNO calibration based on MC simulation result. The full absorption peak of delay signal of neutron capture at Hydrogen (2.22 MeV) is determined as the energy scale. Then we can reconstruct energy of other calibration source with PE/scale. The reconstructed energy is different from true energy due to energy non-linearity. The ratio of reconstructed energy and true energy will be described as energy dependent of non-linearity.

4.2 Relationship between gamma and electron

However, IBD events is positron events. So we would like to know the response of positron energy non-linearity. The relation between gamma and electron can be established with Geant4. And we assume that electron and positron have almost same action of energy non-linearity in addition to two gammas from positron annihilation. There are mainly three physics process for the conversion from gamma to electron, including pair production, Compton scattering, photoelectric effect. Based on the MC simulation, we can obtain the probability density function (PDF) of electron energy with mono energy gamma.

4.3 Model of energy non-linearity

Referring to Daya Bay's method in Ref. [3], an empirical formula with 4 parameters was used to describe energy non-linearity of electron,

$$\frac{E_{vis}}{E_{true}} = \frac{P_0 + P_3 E_{true}}{1 + P_1 e^{-P_2 E_{true}}}. \tag{1}$$

The energy non-linearity of gamma can be deduced with both the empirical formula and the PDF of electron energy.
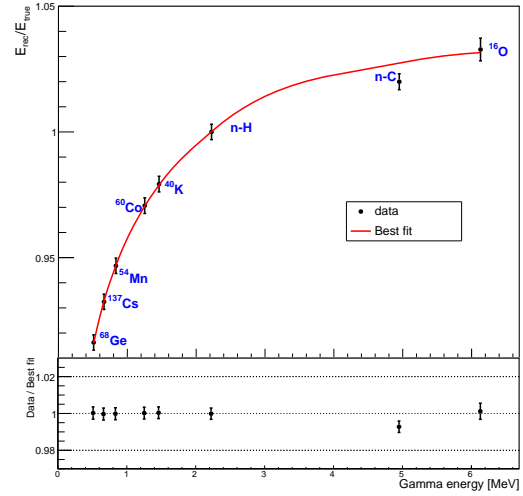

Fig. 6. Fit to data with Eq. (1). The top figure show the non-linearity of gamma with ratio of True energy and reconstructed one. The black point is data from calibration of gamma, while the red line shows the best fit with Eq. (1). The bottom is the ratio of Data and best fit. The error bar is the combination of uncertainties including optical shadowing, Compton effect, electronic non-linearity and statistic.
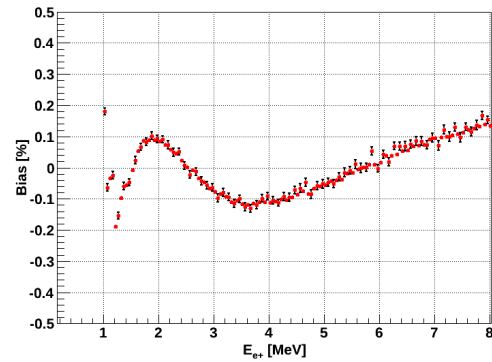

Fig. 7. Bias of positron non-linearity. The non-linearity of positron is obtained by fitting data of gamma non-linearity. And then comparing the reconstruted non-linearity and true non-linearity in MC simulation, we get the bias of two.

4.4 Energy non-linearity of positron

The data of gamma energy non-linearity can be obtained from calibration. With the model we have established, we can fit the data to extract the parameters. Then we get the non-linearity of electron. The only different between electron and positron is annihilation gamma. And this effect can be calibrated with Ge68, ignoring annihilation in flight. The Fig. 6 shows the result of fitting with the model of energy non-linearity.
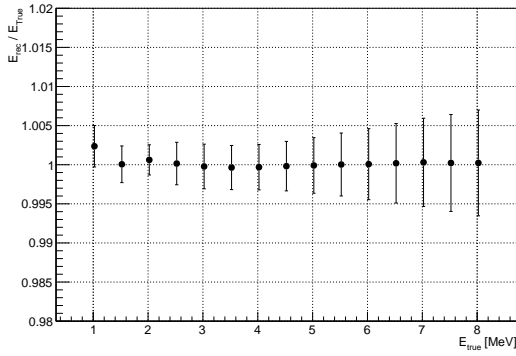

Fig. 8. Systematic uncertainty analysis. The ratio of reconstructed energy and true one shows the bias of non-linearity after calibration for positron. The error bar show the uncertainty. The overall uncertainty of non-linearity is less than 1% from 1 to 8 MeV, which meets the physics requirement of MH determination.
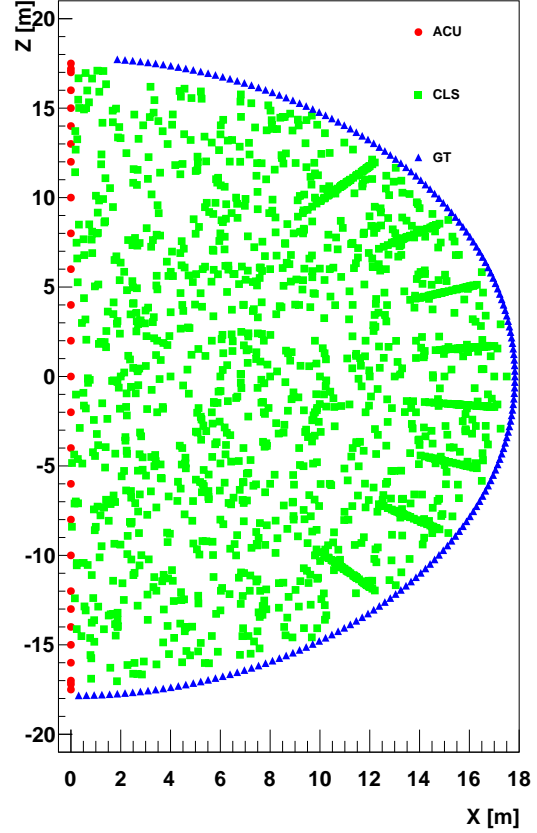

Fig. 9. Calibration mapping. In order to construct to a better strategy of calibration, first we simuate enough calibration points in the half vertical plane. The points is randomly distribute in the plane. Then we will do optimization based on this mapping.

4.5 Systematic uncertainty analysis

Then we consider the uncertainty from optical shadowing effect, Compton tail, statistic effect and electronic non-linearity effect. The true energy scale could be obtained with ideal source in the MC simulation. Then the uncertinty can be randomly added for every source based on the study for every type of effect. Based on the biased energy scale, the non-linearity of positron will be reconstructed. And repeat this procedure multiple times, then we can get the uncertainty of non-linearity compared with the true one as shown in Fig. 8.

5 Energy resolution

The task of calibation is not only for non-linearity but also non-uniformity. The non-uniformity of detector should be corrected with calibration system to contol the energy resolution better than 3%.

With calibration system of CLS, sources can be deployed in one vertical plane. Assuming the response of detector is phi symmetrical, we can do the non-uniformity correction with the vertical calibration mapping. The calibration mapping is shown in Fig. 9. We use one thin plate spline function to fit the data to describe the non-uniformity, as shown in Fig. 10. The function shows the corresponding ratio to CD center. With algorithm of vertex reconstruction, we can get the vertex of IBD events. Then we can correct the non-uniformity by scaling it to CD center. Then we do simulation to qualify the non-uniformity. The mono energy positron uniformly generates in CD. Fig. 11 a shows the energy spectrum of positron, which shows bad energy resolution. Then with the calibration mapping, we can correct it. Fig. 11 b is the energy spectrum after correction, showing better energy resolution with fiducial volume cut R ¡ 17.2 m. We fit the spectrum with Gaussian function to obtain full absorption peak and sigma, then energy resolution can define as sigma/mean. So we use the energy resolution to qualify the non-uniformity correction.
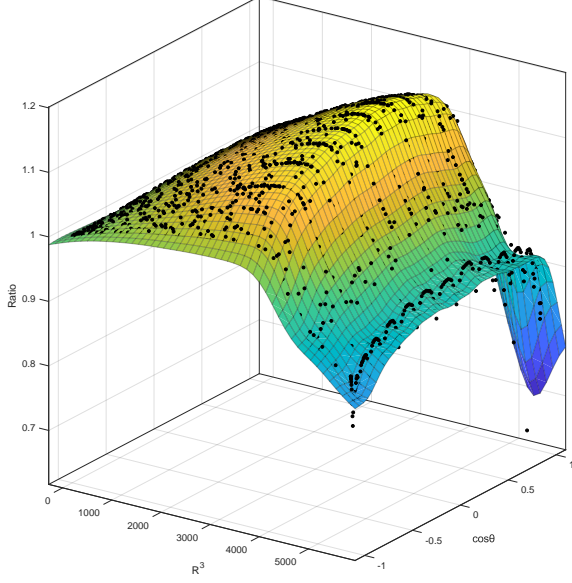

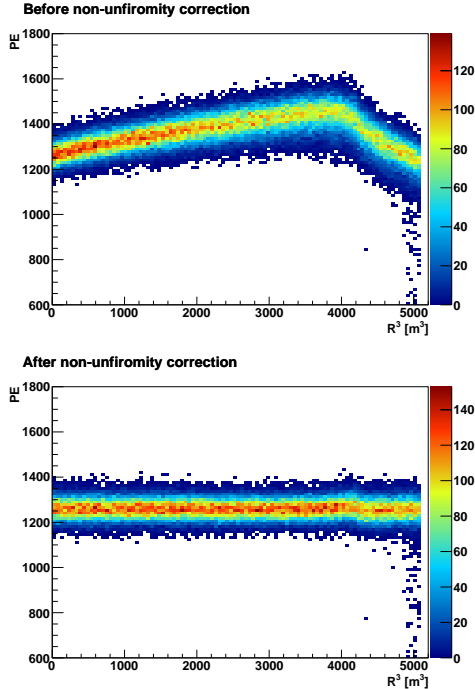Fig. 10.   Spline function to describe the non-uniformity.

Fig. 11.   Non uniformity correction. 0 MeV e+ uniformly distribute in CD. The spline function is used to correction the non-uniformity based on the true vertex for every event.
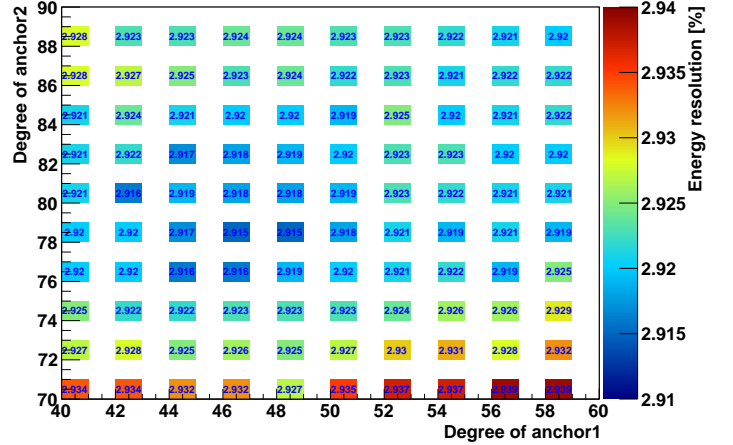

Fig. 12.   Energy resolution as function of two anchors positions. The best choices are respectively 48 degree and 78 degree based on energy resolution.

5.1   Best CLS anchor determinations.

In order to maximize scanning area of calibration, we try to use two asymmetrical CLSs to deploy the source. Therefore, we need to determine the positions of two anchors. Due to self-weight, the cable is not straight, so the source cannot be deployed to the boundary of detector. And in this study, we naively assume the slope angle of cable is 10 degrees as you can see the figure. Varying the two anchor position, we construct different calibration mappings. Then calculate the corresponding energy

resolution. Fig. 12 shows the energy resolution as function of anchor positions. From the calculation, we get the best choice of anchor position (48,78) corresponding minimum energy resolution 2.915%.
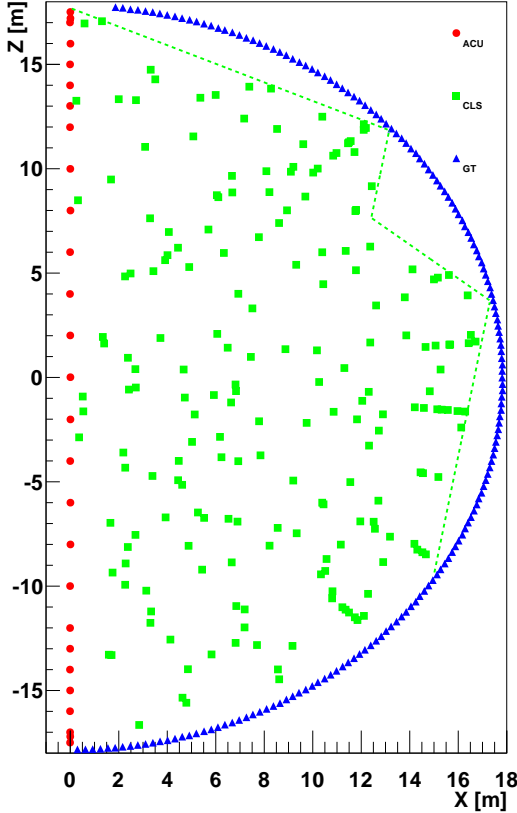

Fig. 13. basic converage with ACU, CLS and GT

5.2 Basic source coverage.

In the realistic experiments, it's impossible to use infinite points to do calibration. We purpose to do the CLS calibration monthly, and to avoid affect the normal physics data taking, the monthly calibration time should be limited to about 1 days. So the inner calibration points are 240, including 21 with ACU and 219 with CLS. We randomly select 219 points from a mount of points, and then calculate the corresponding energy resolution. Repeat the selection multiple times and then get the distribution of energy resolution. Choose the best selection with minimum energy resolution. Fig. 13 shows relative best choice of calibration points.

5.3 Systematic uncertainty analysis.

Vertex reconstruction. The non-uniformity correction depends on vertex of events, so vertex reconstruction significantly affects the quality of non-uniformity correction. Here we use the assumption of vertex reconstruction in Ref. [1], 8 cm @ 1MeV. As shown in table 2, with vertex smearing, the overall energy resolution is 0.02% worse than before. We also assume different vertex reconstruction 10 cm/$\sqrt{E(MeV)}$ and 15 cm/$\sqrt{E(MeV)}$, and get corresponding energy resolution 2.94% and 2.96%.
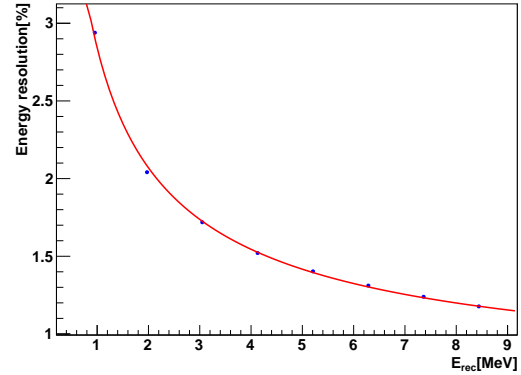

Fig. 14. a=2.75% and b=0.70%, and the overall energy resolution is 2.97%

Positioning smearing. Due to self-weight of cable and friction, it's difficult to determine position of source only based on length of cable. So an independent positioning system was purposed. In this simulation, we assume the accuracy 3 cm, which is the requirement for positioning system. To simulate this effect, we randomly smear the calibration source with 3 cm position resolution. With position smearing for CLS calibration source, the overall energy resolution is 2.94%, 0.01% worse than before as shown in Fig 14.

Table 2 is a summary of energy resolution with different facts. The PMT dark noise is not inclued in this simuation, but we can roughly estimate the value in Ref [1].

6 Conceptual calibration strategy

The conceptual calibration strategy is based on above simulation result. There two types for the routine calibration, weekly calibration and monthly calibration.

6.1 Weekly calibration

The weekly calibration will be operated every week with one radioactive source and one laser, as shown in table 3. The weekly calibration can monitor the variation of energy scale. During the weekly calibration, only ACU will be executed.

6.2 Monthly calibration

The monthly calibration will be operated every month. During the monthly calibration, the ACU, CLS,

and GT will be operated in table 4. The monthly cali-   bration can correct the detector non-uniformity.

Table 2.   Energy resolution with various factors

Effects	a	b	c	$\sqrt{a^2 + (1.6b)^2 + (\frac{c}{1.6})^2}$
ideal	2.693(5)	0.699(5)	0	2.92(1)
vertex smearing	2.707(6)	0.707(5)	0	2.93(1)
positioning precision	2.75(1)	0.70(1)	0	2.97(1)
dark noise	2.75(1)	0.70(1)	0.9	3.02(1)

Table 3.   Time of weekly calibration

Source	Energy [MeV]	PE	Points	Travel time [min]	Date taking time [min]	total time [min]
Neutron (Am-C)	2.22	2990	21	133	105	238
Laser	/	1000 - 8000	6	67	36	103
Total	/	/	/	200	141	341

Table 4.   Time of monthly calibration

System	Source	Points	Travel time [min]	Date taking time [min]	total time [min]
ACU	Neutron (Am-C)	21	133	105	238
CLS	Neutron (Am-C)	219	340	1095	1435
GT	Neutron (Am-C)	11	40	55	95
Total	/	/	/	/	1768

7   Conclusion

Based on the calibration system developed with ACU, CLS and GT, the simulation shows that the strat-egy can satisfy the physics requirement of neutrino MH determination.

Appendices A

References

1 Fengpeng An et al. 2016 . Phys. G: Nucl. Part. Phys. 43 030401

2 Y. Zhang et al. 2019 JINST 14 P01009
3 F. P. An et al. 2014 Phys. Rev. Lett. 112, 061801
4 Jia-Hua Cheng et al. arXiv 1603.04433